A SIMPLE GENERATIVE MODEL OF TRILOBITE SEGMENTATION AND GROWTH

Melanie J. Hopkins[1]

[1]Division of Paleontology (Invertebrates), American Museum of Natural History, Central Park West at 79th Street, New York, NY, 10024, USA. mhopkins@amnh.org

Abstract

Generative growth models have been the basis for numerous studies of morphological diversity and evolution. Most work has focused on modeling accretionary growth systems, with much less attention to discrete growth systems. Generative growth models for molting organisms, such as arthropods, have remained particularly elusive. However, our understanding of post-embryonic growth in trilobite species is sufficiently mature that it is now possible to model growth in a way that incorporates the addition of new parts as well as differential growth rates for existing parts across the trilobite body plan. Furthermore, body size data for a large sample of specimens of the trilobite species *Aulacopleura koninckii* (Barrande, 1846) make it possible to generate robust estimates for model parameters. Although the generative model described here was based on a relatively simple segmentation schedule, a diverse array of observed body sizes and relative proportions of body regions can be attained by altering only a few parameters at a time. Notably, small changes in growth rates can have large effects on body size (e.g. an increase of 4% increases body size by 350%). Subsampling of the empirical dataset indicates that parameters describing the growth gradient in the trunk are more sensitive to sample size than input parameters. Increasing the number of stages represented improves parameter estimates more quickly than increasing number of specimens per stage.

Keywords: trilobites, theoretical morphology, growth model, growth rates, development

This is a preprint that will be submitted to PCI Paleo (https://paleo.peercommunityin.org/) for peer review.

Introduction

Generative growth models have long attracted biologists and mathematicians. Some of the earliest work focused on the geometric form of coiled invertebrates, such as gastropods (e.g., Thompson 1942). In particular, the work by David Raup (Raup 1961, Raup 1966) was foundational for subsequent studies of morphology using model-based descriptors (Hopkins and Gerber 2017). Although generative models for many types of organisms have since been proposed (see McGhee 1999, McGhee 2015 for examples), arthropods have remained elusive, as "discrete growth systems are more difficult to model than accretionary growth systems. Perhaps the ultimate nightmare of any modeler of morphogenesis is organisms that molt, whose entire skeleton is episodically shed and regrown, often with the new skeleton possessing parts or elements not previously present in the organism" (McGhee 1999, p. 142).

Trilobites are an extinct group of marine arthropods with one of the best fossil records of any arthropod group. In part, this is due to the fact that the trilobite dorsal exoskeleton was highly impregnated with low-magnesium calcite (Wilmot and Fallick 1989). Because trilobites started biomineralizing the exoskeleton at very early post-embryonic stages, the growth and morphological development of many species can be pieced together from samples that include fossilized exuviae as well as individual body fossils (Hopkins 2017). With enough well-preserved specimens, it is possible to chart segmentation patterns and estimate growth rates. Segmentation and growth patterns in trilobites are now sufficiently well understood (e.g., Hughes 2003a, Hughes 2003b, Minelli et al. 2003, Hughes 2005, Hughes et al. 2006, Hughes 2007, Minelli and Fusco 2013, Fusco et al. 2014, Hong et al. 2014, Fusco et al. 2016) that generative growth models are within reach. Further, measurements of body size and body proportions for a large sample of specimens are now available for one of the best studied trilobite species in this regard, *Aulacopleura koninckii* (Barrande, 1846) (Hughes et al. 2017). In this paper, I use these studies as a basis for developing a simple generative model for trilobites and explore the impact of varying different parameters on body size and body proportions.

Segmentation patterns and growth during trilobite ontogeny

Like some centipedes and most crustaceans, the final segmental composition of the trilobite body was attained during post-embryonic ontogeny through a series of molts (Fusco and Minelli 2013). Trilobites had a hemianamorphic mode of segmentation, meaning they underwent a phase of molts during which new segments were added to the body followed by a phase during which molting continued without further increase in the number of body segments (Minelli et al. 2003, Minelli and Fusco 2013). In

trilobites, the earliest biomineralized molt was a single articulated sclerite comprised of some number of fused segments; this has been termed the protaspid period. The subsequent meraspid period began when molting resulted in the first articulation between the cephalon and the transitory pygidium, each comprised of fused segments. During subsequent molts, either new segments were generated near the posterior end of the transitory pygidium, or a new articulation appeared at the anterior end of the transitory pygidium (i.e., a thoracic tergite[1] was released into the thorax), or both. At some point, segment generation ceased (ending the anamorphic phase and initiating the epimorphic phase) and articulation generation ceased (ending the meraspid period and initiating the holaspid period). The relative timing of these transitions varied across species, and three different schedules have been documented in trilobites: 1) hypoprotomeric, where individuals entered the epimorphic phase within the meraspid period (the cessation of new segment generation preceded the cessation of new thoracic articulation); 2) synanthromeric, where individuals entered the epimorphic phase and holaspid period synchronously; and 3) protarthrous, where individuals entered the epimorphic phases within the holaspid period (the cessation of new thoracic articulation preceded the cessation of new segment generation in the pygidium) (Hughes et al. 2006).

During the meraspid period, the number of tergites in the thorax is a size-independent measure of relative age of the individuals. Per-molt size increase was constant for some sclerites for some portions of the ontogeny in at least some trilobites (Chatterton et al. 1990, Fusco et al. 2012), but detailed data-rich studies of the trilobite *Aulocopleura koninckii* indicate that the rate of growth in the thorax was governed by a growth field described by a continuous gradient rather than constant per-tergite rates (Fusco et al. 2014, 2016).

Description of the growth model

Because total body size at any given point during ontogeny (as well as potential maximum body size) was determined both by the segmentation schedule and the pattern of growth rates, several parameters are needed in order to model trilobite growth. Parameters are summarized in Table 1. An R function for running the growth model using these parameters is available at www.github.com/meljh/trilo-growth.

---

[1] Traditionally, the articulated sclerites in the thorax of the trilobite exoskeleton have been called "thoracic segments". Throughout this manuscript, I refer to the thoracic segments as "tergites" to reflect their anatomical similarity to other arthropods and distinguish them from body segments, which may not be positionally synchronous (Ortega-Hernández and Brena 2012)

Cephalic growth

Growth rate of cephalon (*g.c*). Although the relative size of features on the cephalon (e.g., the length of the glabella relative to the length of the cephalon) changes during ontogeny (Fusco et al. 2016, Hopkins and Pearson 2016, Hopkins 2017), this model assumes that the growth rate of the cephalon as a whole was constant (Chatterton et al. 1990, Fusco et al. 2012). For each molt *M*, the size of the cephalon is estimated as *ce * g.c^M* where *ce* is the initial size of the cephalon at M0 (see below) and *g.c* is the growth rate.

==Defining the growth gradient of the trunk==

Fusco et al. (2014) found that an exponential decay function best described the distribution of per-molt local growth rates across the trunk during the meraspid period, specifically that the growth at relative position x along the trunk = $a + b*\exp(-\lambda(1-x))$. When $x = 0$, this equation simplifies to growth rate = a; this is the lower bound for the growth gradient (*lowM* in Table 1). When $x = 1$, the equation simplifies to growth = $a + b$; this sum is the upper bound for the growth gradient (*highM* in Table 1). The exponential decay constant (λ) describes the concavity of the exponential decay curve, and is represented in the model by the parameter *lambdaM* (Table 1). Because the growth gradient may shift during the transition from the meraspid to holaspid stages (Fusco et al. 2016), three additional parameters are included to describe the holaspid growth gradient (*lowH*, *highH*, and *lambdaH* in Table 1).

This gradient includes the pygidium, but newly released tergites were sourced from the anterior region of the growing transitory pygidium. Therefore the model effectively takes the following steps to determine the lengths of the tergites and transitory pygidium in each subsequent molt during the meraspid period:

1. Determine the relative position along the trunk of the median points of each tergite and on the transitory pygidium at the preceding molt.
2. Sample the exponential decay function at these relative positions to generate a vector of growth rates along the trunk.
3. Apply these rates to the respective lengths of each tergite and the transitory pygidium.

At this point the new length of the "pygidium" is the sum of the length of the new transitory pygidium and the length of the newly released tergite. Therefore the following additional steps are required:

4. Assign a length to the newly released tergite (see below).

5. Determine the length of the new transitory pygidium by subtracting the length of the newly released tergite.

For the holaspid period, the model follows steps 1 – 3 for each molt.

Parameters determining initial input and transition points

Number of molts in lifespan (*N*). The number of molts determines the number of time-steps in the model. The only restriction on this parameter is that it must be greater than the number of molts during the meraspid period (*Ter*).

Number of molts during meraspid period (*Ter*). For most trilobite species, a thoracic tergite was released at each molt during the meraspid period. Thus this parameter will be equal to the terminal number of thoracic tergites for most species. The model currently does not accommodate exceptions (such as molts accompanied by no tergite release or multiple tergite release), although this could be modified in the future. In the model, when $N < Ter$, the parameters describing the growth gradient change are those defined for the meraspid period; when $N \geq Ter$, the parameters describing the growth gradient are those defined for the holaspid period (see above).

Length of cephalon and transitory pygidium at M0 (*ce* and *p*, respectively). These parameters describe the size of the trilobite at the onset of epimorphic growth, where M0 refers to the molt characterized by one articulation between the cephalon and the transitory pygidium. These parameters set the initial size of the trilobite and can be estimated directly from fossil specimens or estimated from growth series.

Length of newly released tergite (*t.p*). This parameter determines the size of the tergite released from the transitory pygidium at each molt during meraspis. Because the new tergite was sourced from the anterior region of the pygidium, the length of the newly-released tergite may be defined as a proportion of the pygidial length after the growth gradient has been applied.

Number of molts during which initial or "meraspid" growth gradient is active (*R*). It is possible that the growth gradient did not always transition at the start of holaspis, especially for protarthrous species. This parameter defines the number of molts for which the initial growth gradient was still active. It is thus constrained to range from zero to *N*. If $R < Ter$, then the change in growth rates occurs before the last tergite is released. If $R > Ter$, then the change in growth rates occurs after the last tergite is released. If $R = Ter$, then there is no transition to a new growth gradient. It is possible that the growth gradient changed

gradually throughout ontogeny. This is not accommodated in the current model but could be potentially accommodated in the future by defining vectors of molt-dependent growth rates.

Parameter estimates from empirical data

I used a data set of measurements from *Aulacopleura koninckii* specimens (Hughes et al. 2017) to estimate values for each model parameter.

Cephalic growth rate ($g.c$). The growth rate for both species was estimated using the slope of the OLS regression of logged cephalic lengths against the number of tergites in the thorax for all specimens certain to be meraspids[2]. For *Aulacopleura koninckii*, lines were fit to juvenile stages 9-17 (N = 137) because the number of specimens representing earlier stages were too few (N = 11), following Fusco et al. (2014) (Fig. 1A).

Meraspid growth gradient. The number of tergites provides a size-independent measurement of age during the meraspid stage. For meraspids, model parameters a, b, and λ were estimated by fitting an exponential curve to average per-molt tergite growth rates against relative tergite position in the trunk. The relative position in the trunk of the posterior margin of each tergite was calculated by scaling the cumulative average lengths of the trunk sclerites to range from 0 to 1 and then finding the midpoint of each tergite along this range. Growth rates between stages were calculated by dividing the average tergite lengths in stage $i + 1$ by the averages in stage i. For *Aulacopleura koninckii*, curves were fit to juvenile stages 9-17 (N = 137) because the number of specimens representing earlier stages were too few (N = 11), following Fusco et al. (2014).

Holaspid growth gradient. Unlike meraspids, holaspids are characterized by having the same number of tergites, so this trait cannot be used as a size-independent measure of age. However, because cephalic growth rates are assumed to be constant across ontogeny, holaspids can be assigned to molt stages by extrapolating from an OLS regression of ln(cephalic length) against molt stage from meraspid specimens (Fusco et al. 2016). Model parameters a, b, and λ are then estimated in the same fashion as for the meraspid growth gradient. *Aulacopleura koninckii* has a variable number of terminal segments, ranging from 18 to 22 and yielding 5 holaspid morphotypes. Note that *A. koninckii* provides an unusual case study for trilobites in having had a variable terminal number of thoracic tergites. For most species there appears

---

[2] *Aulacopleura koninckii* had a variable number of terminal thoracic tergites, ranging from 18 to 22 (see section "Holaspid growth gradient" for further discussion). Therefore only specimens with 17 or fewer segments are certain to be meraspids.

to be no variation, and in some clades the terminal number of tergites was highly conserved (e.g., Lichidae species had 11 tergites at the onset of epimorphosis, Thomas and Holloway 1988, Whittington 2002).

Fusco et al. (2016) found that growth gradients were similar among holaspid morphotypes; for this study, parameters were estimated using specimens with 20 tergites because this is the median terminal number of thoracic tergites achieved by *A. koninckii* individuals. Growth gradient curves are shown in Figure 1B.

Number of molts in lifespan (*N*). The total number of molts was set to the maximum estimated holaspid stage (see "Holaspid growth gradient" above).

Number of molts during meraspid period (*Ter*). The total number of molts during the meraspid stage was set to 20 for *Aulacopleura koninckii*, which is the median terminal number of thoracic tergites achieved by *A. koninckii* individuals.

Length of cephalon and transitory pygidium at M0 (*ce* and *p*, respectively). In order to estimate initial size parameters, the length of the cephalon at M0 was set as the intercept of the same regression used to determine the cephalic growth rate (see above and Fig. 1A). Because new tergites were released from the anterior part of the transitory pygidium during the meraspid phase, the average length of the pygidium stayed generally constant (Fig. 1C). Thus the length of the transitory pygidium at M0 was set as the average across all meraspids.

Length of newly released tergite (*t.p*). This parameter was estimated as the average ratio between the length of newly released thoracic tergite in each meraspid molt (for all individuals with 17 or fewer tergites) relative to the sum of that length and that of the pygidium in the same molt (Fig. 1D). It is possible that some of the variation in this ratio across specimens (and that of pygidial length through ontogeny) is due to variation in the number of segments expressed in the transitory pygidium in different individuals with the same number of tergites. However, there is no consistent relationship between the number of segments in the transitory pygidium and its length (Supplementary Figure 1).

Number of molts during which initial or "meraspid" growth gradient is active (R). Because *Aulacopleura koninckii* is synanthromeric, this parameter is set to equal the number of molts during the meraspid period (*Ter*).

Table 1. Parameters (all single variables) that can be adjusted in the model and parameter estimates for *Aulacopleura koninckii* (based on data from Hughes et al. 2017). An R function for calculating these estimates from the dataset is available at www.github.com/meljh/trilo-growth.

Parameter	Description	Parameter estimates for *A. koninckii*
N	Number of molts in lifespan	31
Ter	Number of molts during meraspid period	20
ce	Length of cephalon at M0	0.671
p	Length of transitory pygidium at M0	0.549
t.p	Length of newly released tergite, as proportion of pygidial length in previous stage	0.182
R	Stage at which rates transition from "initial/meraspid growth gradient" to "final/holaspid growth gradient"	20
lowM	Minimum growth rate (of growth gradient) for thorax during meraspis ($\pm R$); equivalent to *a* in exponential decay function	1.059
highM	Maximum growth rate (of growth gradient) for thorax during meraspis ($\pm R$); equivalent to *a* + *b* in exponential decay function	1.370
lambdaM	Exponential decay constant defining growth gradient during meraspis ($\pm R$); equivalent to λ in exponential decay function	5.001
lowH	Minimum growth rate (of growth gradient) for thorax during holaspis (or post-*R*); equivalent to *a* in exponential decay function	1.084
highH	Maximum growth rate (of growth gradient) for thorax during holaspis (or post-*R*); equivalent to *a* + *b* in exponential decay function	1.168
lambdaH	Exponential decay constant defining growth gradient during holaspis (or post-*R*); equivalent to λ in exponential decay function	5.806
g.c	Growth rate of cephalon, assumed constant throughout lifespan	1.085

Output of the model for *Aulacopleura koninckii*

The output of the model is the estimated lengths of each dorsal sclerite at each molt. The output after applying the parameters calculated from measurements of *Aulacopleura koninckii* is shown in Figure 2. Modeled body sizes and body proportions are similar to empirical data for *A. koninckii* (Table 2). However, in the model output, the length of the thoracic tergites decrease posteriorly in the trunk at all molt stages. In the empirical dataset, the length of the thoracic tergites tends to increase posteriorly for the first four or five segments before decreasingly to the pygidium (there is variation in this, but it is not clear how much might be due to measurement error), a pattern that has been seen in other trilobites as well.

Table 2. Comparison of length estimates from model to length estimates from empirical data (Hughes et al. 2017). Assuming a constant cephalic growth rate, the largest specimen with 20 terminal segments in the empirical dataset is estimated to have molted 31 times (based on OLS regression of log(cephalic size) on molt stage in juveniles) and should be comparable to the model output at molt 31.

Length	Model output (mm)	Average from empirical data (mm)
Cephalon, molt 9	1.40	1.42
Cephalon, molt 14	2.10	2.06
Cephalon, maximum	8.40	8.36
Transitory pygidium, molt 9	0.46	0.56
Transitory pygidium, molt 14	0.52	0.54
Pygidium, maximum	3.02	2.46
Thorax, molt 9	1.49	1.30
Thorax, molt 14	2.92	2.52
Thorax, maximum	16.06	13.90
Total body size, molt 9	2.86	2.72
Total body size, molt 14	5.02	5.11
Total body size, maximum	27.48	24.72

Parameter variation and resulting relative growth

The relative length of different sclerites, as well as maximum body size, may be explored by varying different parameters:

Influence of varying the initial cephalic and pygidial length. It is likely that there was variation in the size of the cephalon and transitory pygidium at M0. In order to capture the influence of this variation on total body length, the initial cephalic and pygidial lengths were sampled from normal distributions with means of 0.67 and 0.55, respectively, and standard deviations of 0.05. When the lengths of the cephalon and

transitory pygidium at M0 are allowed to vary, the variance in body size at any given molt increases through growth (Figure 3). This puts a fine point on the fact that there is no canalization mechanism built into the current model (see Hughes et al. 2017for discussion of growth canalization).

Influence of varying the number of terminal tergites in the thorax. If no other parameters are changed, one might expect that reducing the number of tergites will result in smaller trilobites. This is true, but the decrease is small. For example, decreasing the number of terminal thoracic tergites by 50% (Ter =10) results in a trilobite that is only 85% smaller (Figure 4). Because the cephalon is growing at the same rate, it is the relative proportions of the trunk that vary to accommodate this. In particular, the relative length of the pygidium is much greater in a trilobite with fewer thoracic tergites because the pygidium is under positive growth (during which it no longer releases tergites into the thorax) for a greater proportion of the lifespan. In addition, any particular tergite numbered from the front (e.g., the second tergite) will undergo a relatively higher growth rate throughout the lifespan because it shares a larger portion of the growth gradient. However, smaller (and re-proportioned) trilobites would result if there was a limit on the total number of molts a trilobite underwent during holaspis $(N < 31)$ rather than a limit on the total number of molts during the entire lifespan.

Influence of increasing rates systematically across body regions. It should be possible to generate a smaller or larger trilobite without altering body proportions if rates are adjusted systematically across all body regions. To determine the sensitivity of body size to changes in rates, the cephalic growth rate ($g.c$) and the minimum and maximum growth rates of the trunk region ($lowM, highM, lowH, highH$) were systematically adjusted and the model re-run. A four-percent increase in the rates across these five parameters results in a trilobite that is 3.5 times larger than before but with the same relative body proportions (Table 3).

Table 3. Increase in total body size if growth parameters are systematically increased. The cephalic and pygidial lengths are relative to the total body size.

Proportional change in each parameter	g.c	lowM	highM	lowH	highH	Total body size (mm)	Relative cephalic length	Relative pygidial length
1	1.085	1.060	1.370	1.084	1.168	27.48	0.306	0.110
1.01	1.096	1.070	1.383	1.095	1.180	37.41	0.306	0.110
1.04	1.128	1.102	1.425	1.127	1.215	92.69	0.306	0.110
0.99	1.074	1.049	1.356	1.073	1.156	20.12	0.306	0.110
0.96	1.042	1.017	1.315	1.040	1.121	7.75	0.306	0.110

<u>Influence of varying the growth gradient during meraspis or holaspis</u>. In *A. koninckii*, the growth gradient becomes shallower at the transition from the meraspid period to the holaspid period, due to an increase in the minimum and decrease in the maximum rates (Figure 1B).

The maximum rates along the growth gradient (*highM, highH*) primarily affect growth of the pygidium, and this transition also marks the point in growth where the pygidium actively increases in size because tergites are no longer being released into the thorax. Thus, one way to make an isopygous trilobite (one where the pygidium is of equal length the cephalon) is to maintain the high growth rate at the posterior part of the trunk into holaspis, for example by retaining the meraspid growth gradient through holaspis (Figure 5). One interesting result is also that the length of the thoracic tergites decreases and then increases posteriorly in the latest molt stages. The pygidium will eventually outgrow the cephalon if λ is increased during the holaspid period, which would decrease the concavity of the exponential decay curve and result in higher growth rates across a larger area of the posterior part of the trunk.

The holapsis growth curve in *A. koninckii* is shallow enough along most of the trunk that the relative length of the thorax remains almost constant during holaspis (Figure 2, 4). As the range of the growth gradient is decreased, the exponential curve becomes more and more similar to a horizontal line. This ultimately results in true isomorphic growth along the trunk (i.e., constant rates rather than a growth gradient) (Figure 6). Because of the shape of the exponential decay curve, a constant rate near the lower end of the growth gradient (1.084 for *A. koninckii*) yields a total body length closest to that of actual specimens, but the relative length of the pygidium to the cephalon is much smaller. Further, because the minimum growth rate of the trunk (*lowH*) is almost exactly the same as the cephalic growth rate, the relative proportions of the cephalon, thorax, and pygidium will remain constant during holaspis when the holaspid rates are constant and low (Figure 6G-I).

<u>Influence of decoupling between timing of shift in growth gradients and termination of tergite release</u>. Because the growth gradient is shallower and has a smaller maximum rate during holaspis than during meraspis (at least in *A. koninckii*), altering the timing of transition between growth gradients has differential effects depending on whether the transition between growth gradients occurs before or after termination of tergite release (Figure 7, Table 4). If the transition happens earlier in ontogeny relative to the termination of tergite release, the total exoskeletal length is slightly smaller because rates decrease sooner but the pygidium is much smaller because tergite release continues even though the pygidium grows at a slower rate. In contrast, if the transition happens later in ontogeny relative to the termination of tergite release, the total exoskeletal length is slightly larger but the pygidium is much larger because high

growth rates continue even after tergites are no longer being released. The change in relative proportions would not be as great if new segment generation occurred in the thorax as opposed to the pygidium.

Table 4. Comparison of exoskeletal proportions when growth gradient shift occurs before, coincident with, or after termination of tergite release into the thorax. In this example, termination of tergite release occurs at molt 20 ($Ter = 20$). All length measurements are standardized to $R = 20$ ($R = Ter$).

R	Relative total length	Relative length of thorax	Relative length of pygidium
15 ($R \ll Ter$)	0.928	0.960	0.559
18 ($R < Ter$)	0.963	0.986	0.740
20 ($R = Ter$)	1	1	1
22 ($R > Ter$)	1.017	0.990	1.214
24 ($R \gg Ter$)	1.044	0.967	1.574

How many specimens are needed to estimate growth parameter?

The *Aulacopleura koninckii* of dataset of Hughes et al. (2017) comprises 351 well-preserved articulated specimens, 40% of which span the ontogeny of the species from meraspid stage 4 to 17 (sample sizes for each stage shown in Supplementary Figure 1). Such a collection of specimens is exceedingly rare, for both taphonomic and practical reasons. Thus, it may be useful to know how many specimens are needed to accurately estimate growth parameters for this and other species, and what level of precision might be expected under different sampling scenarios. Subsampling routines of the *A. koninckii* dataset produced the following results.

One specimen per stage. One specimen per stage (M9-M17) was randomly selected from the dataset and the following parameters were estimated: 1) the cephalic length at M0 (*ce*); 2) the transitory pygidium length at M0 (*p*); 3) the rate of growth of the cephalon (*g.c*); 4) the proportional size of the newly released tergite at each stage (*t.p*); and 5) the minimum (*lowM*), maximum (*highM*), and exponential decay constant (*lambdaM*) describing the growth gradient. This was repeated 1000 times. In each iteration, each stage was represented by one specimen.

All of the input parameters (*ce,* Figure 8A; *p*, Figure 8B; *g.c*, Figure 8C, *t.p,* Figure 8D) are well estimated, while the minimum and maximum growth rates in the trunk (*lowM,* Figure 8E, *highM*, Figure 8F) tend to be overestimated, and the exponential decay constant tends to be underestimated (*lambdaM*, Figure 8G. The result of this imprecision on input parameters is expected to be small, given that impact on total body size of varying the initial cephalic and pygidial length (*ce* and *p*) using a higher standard

12

deviation (Figure 3). However, the ranges of values for the growth gradient parameters is high: even excluding the extreme outliers, the range of values is greater than the difference between the meraspid and holaspid growth gradients estimated for *A. koninckii* (Table 1). Given the results of varying these parameters above (Figures 3-7), poor estimates for growth gradient parameters are expected have a greater impact on model output than poor estimates for input parameters.

More than one specimen per stage. *n* specimens were randomly selected from each of stages M9-M17, where *n* ranged from 2 to 8 (8 is the minimum number of specimens representing these stages, see Supplementary Figure 1), and the four input and three meraspid growth parameters were estimated. This was repeated 1000 times. In each iteration, each stage was represented by the same number of specimens. For graphical comparison, univariate density estimates were constructed from the frequency distributions using the sm.density function in the R package *sm* ver. 2.2-5.6 (Bowman and Azzalini 2018).

As expected, with an increase in the number of specimens per stage, the range in parameter estimates decreased (Figure 9). The mean estimates shifted towards values estimated from the entire empirical dataset, most notably for growth gradient parameters which were more severely over- or underestimated at low sample sizes (Figure 9E-G). Here, where specimens were being drawn from the latter half of the meraspid period (M9-M17), at least six specimens per meraspid molt stage were needed to accurately estimate parameters describing the growth gradient. For both input and growth gradient parameters, sampling more than six specimens per meraspid growth stage yielded increasingly precise estimates, but with diminishing returns.

A few specimens from few to many stages. *n* specimens from *k* stages were randomly selected from the dataset and the four input and three meraspid growth parameters were estimated. For the input parameters, this was repeated 1000 times for each of *k* ranging from 3 to 14 (representing just three to all stages M4-M17) and for *n* number of specimens ranging from 3 to 5. Because determining the growth gradient requires a larger sample size (= larger number of molt stages represented), growth parameters were estimated for each of *k* ranging from 10 to 14 (representing ten to all stages M4-M17). In each iteration, each selected stage was represented by the same number of specimens.

As expected, with an increase in the number of stages represented, the range in parameter estimates decreased (Figure 10, 11). However, there was no shift in the mean estimate of growth gradient parameters as the number of stages represented was increased (Figure 11). This implies that once many meraspid stages are represented in a sample (> 10), fewer specimens per stage are required to get accurate estimates. The precision was more quickly improved by increasing the number of stages represented than by increasing the number of specimens (within a small range) in each stage (Figure 11).

Implications and applications of the model

With the approach proposed in this paper, a minimum of nine parameters are required to model basic trilobite growth and segmentation, and three additional parameters are required to allow a transition to a new growth gradient for the trunk region during ontogeny. It is possible to add additional parameters to describe additional variation in the segmentation schedule or variation in growth rates throughout ontogeny. As an example herein, the parameter R allows for variation in the timing of the transition to a new growth gradient. It should also be possible to apply this approach to modeling growth in other arthropods, particularly other hemianamorphic arthropods for which segmentation patterns are known (e.g., conchostracans, Oleson 1999, copepods, Ferrari and Dahms 2007). One of the major obstacles in applying this to other arthropods may be the initial estimation of parameters from empirical data, which requires samples comprising multiple specimens from multiple molt stages (although good representation of molt stages will likely be more important than large numbers of specimens within molt stages).

Although this model describes basic growth and segmentation, a diverse array of observed body sizes and relative proportions of body regions can be attained by altering only a few parameters at a time. Given a set number of molts, small changes in growth rates can have large effects on total body size or relative body proportions. The extent to which such changes (and of this magnitude) are ecologically or evolutionarily possible is an open question. A 50% increase in body size is seen in *Poseidonmicus* ostracods over the last 40 million years in association with a decrease in ocean bottom-water temperatures, and some species exhibit almost this entire range of body size across historic populations (Hunt and Roy 2006). Because ostracods have determinant growth and a fixed number of molt stages, it seems likely that this body size variation was achieved by changes to per-molt growth rates. However, in arthropods with indeterminate growth (like trilobites), variation in adult body sizes in response to environmental variation (e.g., temperature, food availability, presence of predators) is often achieved by some combination of changes in magnitude of per-molt increase in body size and changes in molt frequency and/or number of molts per life history phase (Maszczyk and Brzezinski 2018). Better understanding of growth response to environmental variation in trilobites requires further empirical studies (e.g., comparisons of environmentally-separated populations of the same species). In the meantime, the model proposed herein may provide a framework for assessing the range of realized body sizes and body proportions in trilobites, and for revealing possible ways in which body size and body proportions may have evolved.

Acknowledgements

References

Bowman, A. W., and A. Azzalini. 2018. R package 'sm': nonparametric smoothing methods (version 2.2-5.6). http://www.stats.gla.ac.uk/~adrian/sm.

Chatterton, B. D. E., D. J. Siveter, G. D. Edgecombe, and A. S. Hunt. 1990. Larvae and relationships of the Calymenina (Trilobita). Journal of Paleontology **64**:255-277.

Ferrari, F. D., and H. U. Dahms. 2007. Post-embryonic development of the Copepoda, Crustacean Monographs 8. Brill, Leiden.

Fusco, G., J. T. Garland, G. Hunt, and N. C. Hughes. 2012. Developmental trait evolution in trilobites. Evolution **66**:314-329.

Fusco, G., P. S. Hong, and N. C. Hughes. 2014. Positional specification in the segmental growth pattern of an early arthropod. Proceedings of the Royal Society B: Biological Sciences **281**.

Fusco, G., P. S. Hong, and N. C. Hughes. 2016. Axial growth gradients across the postprotaspid ontogeny of the Silurian trilobite *Aulacopleura koninckii*. Paleobiology **42**:426-438.

Fusco, G., and A. Minelli. 2013. Arthropod segmentation and tagmosis. Pages 197-221 *in* A. Minelli, G. Boxshall, and G. Fusco, editors. Arthropod Biology and Evolution: molecular, development, morphology. Springer-Verlag, Berlin Heidelberg.

Hong, P. S., N. C. Hughes, and H. D. Sheets. 2014. Size, shape, and systematics of the Silurian trilobite *Aulacopleura koninckii*. Journal of Paleontology **88**:1120-1138.

Hopkins, M. J. 2017. Development, trait evolution, and the evolution of development in trilobites. Integrative and Comparative Biology **57**:488-498.

Hopkins, M. J., and S. Gerber. 2017. Morphological Disparity. Pages 1-12 *in* L. Nuno de la Rosa and G. Müller, editors. Evolutionary Developmental Biology: A Reference Guide. Springer International Publishing, Cham.

Hopkins, M. J., and J. K. Pearson. 2016. Non-linear ontogenetic shape change in *Cryptolithus tesselatus* (Trilobita) using three-dimensional geometric morphometrics. PALAEONTOLOGIA ELECTRONICA **19.3.42A**:1-54.

Hughes, N. C. 2003a. Trilobite body patterning and the evolution of arthropod tagmosis. BioEssays **25**:386-395.

Hughes, N. C. 2003b. Trilobite tagmosis and body patterning from morphological and developmental perspectives. Integrative and Comparative Biology **43**:185-206.

Hughes, N. C. 2005. Trilobite construction: building a bridge across the micro- and macroevolutionary divide. Pages 139-158 *in* D. E. G. Briggs, editor. Evolving Form and Function: Fossils and Development: Proceedings of a symposium honoring Adolf Seilacher for his contributions to paleontology, in celebration of his 80th birthday. Peabody Museum of Natural History, Yale University, New Haven.

Hughes, N. C. 2007. The evolution of trilobite body patterning. Annual Review of Ecology, Evolution and Systematics **35**:401-434.

Hughes, N. C., P. S. Hong, J. Hou, and G. Fusco. 2017. The development of the Silurian trilobite *Aulacopleura koninckii* reconstructed by applying inferred growth and segmentation dynamics: A case study in paleo-evo-devo. Frontiers in Ecology and Evolution **5**:00037.

Hughes, N. C., A. Minelli, and G. Fusco. 2006. The ontogeny of trilobite segmentation: a comparative approach. Paleobiology **32**:602-627.

Hunt, G., and K. Roy. 2006. Climate change, body size evolution, and Cope's Rule in deep-sea ostracodes. Proceedings of the National Academy of Sciences **103**:1347-1352.

Maszczyk, P., and T. Brzezinski. 2018. Body size, maturation size, and growth rate of crustaceans. Pages 35-65 *in* G. A. Wellborn and M. Thiel, editors. The Natural History of the Crustacea Volume 5, Life Histories. Oxford University Press, Oxford.

McGhee, G. R. 1999. Theoretical morphology: the concept and its applications. Columbia University Press.

McGhee, G. R. 2015. Limits in the evolution of biological form: a theoretical morphologic perspective. Interface Focus **5**:20150034.

Minelli, A., and G. Fusco. 2013. Arthropod post-embryonic development. Pages 91-122 *in* A. Minelli, G. Boxshall, and G. Fusco, editors. Arthropod Biology and Evolution: molecular, development, morphology. Springer-Verlag, Berlin Heidelberg.

Minelli, A., G. Fusco, and N. C. Hughes. 2003. Tagmata and segment specification in trilobites. Special Papers in Palaeontology **70**:31-43.

Oleson, J. 1999. Larval and post-larval development of the branciopod clam shrimp *Cyclestheria hislopi* (Baird, 1859) (Crustacea, Branchiopoda, Conchostraca, Spinicaudata). Acta Zoologica **80**:163-184.

Ortega-Hernández, J., and C. Brena. 2012. Ancestral patterning of tergite formation in a centipede suggests derived mode of trunk segmentation in trilobites. PLoS ONE **7**:e52623.

Raup, D. M. 1961. The geometry of coiling in gastropods. Proceedings of the National Academy of Sciences of the United States of America **47**:602.

Raup, D. M. 1966. Geometric analysis of shell coiling: general problems. Journal of Paleontology **40**:1178-1190.

Thomas, A. T., and D. J. Holloway. 1988. Classification and phylogeny of the trilobite order Lichida. Philosophical Transactions of the Royal Society of London B **321**:179-262.

Thompson, D. A. W. 1942. On Growth and Form: The Complete Revised Edition. Cambridge University, Cambridge.

Whittington, H. B. 2002. Lichidae (Trilobita): morphology and classification. Journal of Paleontology **76**:306-320.

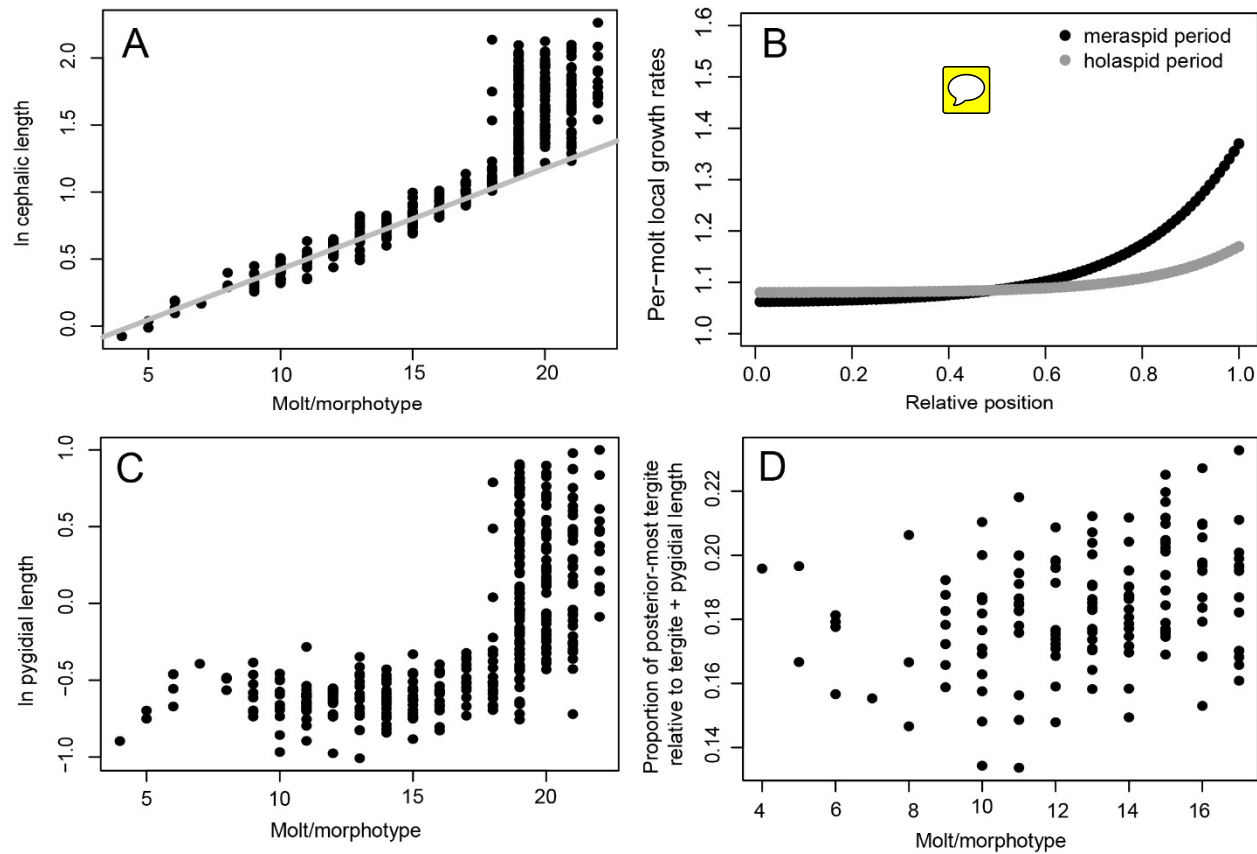Wilmot, N. V., and A. E. Fallick. 1989. Original mineralogy of trilobite exoskeletons. Palaeontology **32**:297-304.

Figure 1. Summary of empirical data used to derive parameter estimates. (**A**) Lengths of cephala in *A. koninckii* grouped by number of tergites in the thorax. Because the terminal number of tergites is variable in *A. koninckii*, the regression line was based only on molts which were clearly within the meraspid phase (number of tergites < 18). The rate of cephalic length increase is the exponential of the slope of the regression line. (**B**) Growth gradients along trunk for *A. koninckii* during the meraspid (black) and holaspid (gray) periods. (**C**) Lengths of transitory and adult pygidia in *Aulacopleura koninckii,* grouped by the number of tergites in the exoskeleton. The terminal number of tergites was variable in *A. koninckii* (ranging from 18 to 22), which is why the average length and range of length measurements increases dramatically at molt/morphotype 18. Note that the size of the transitory pygidium does not change significantly during the meraspid period although there may have been increases and decreases over ontogeny. (**D**) Proportion of the length of the "pygidial" part of the trunk that is expressed as the newly-released tergite in *A. koninckii*. Although the number of segments in each transitory pygidium varies in *A. koninckii*, there is no relationship between the length of the pygidium and the number of segments for any meraspid molt (Supplementary Figure 1).
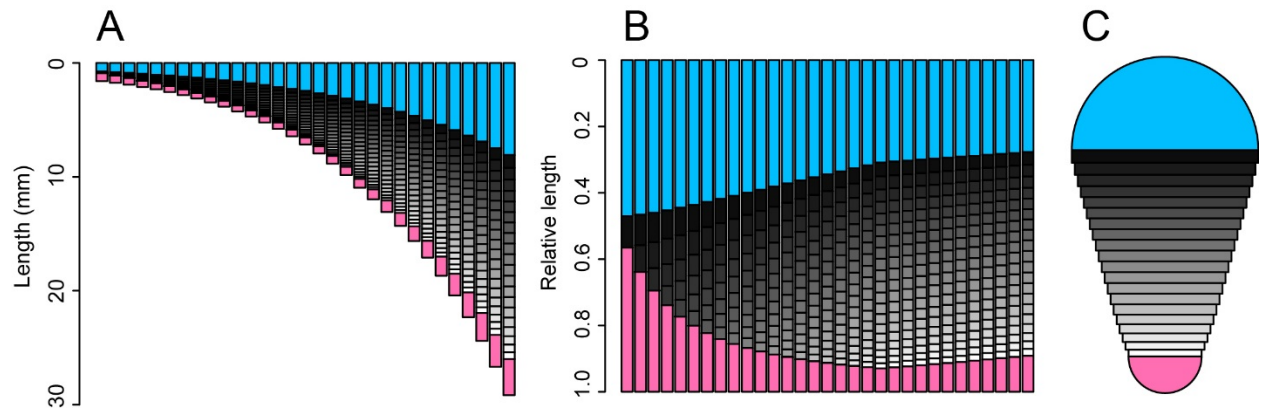
Figure 2. Model results. Estimated (**A**) and relative lengths (**B**) of dorsal sclerites for each molt (up to M = 31) when model is tuned using the parameter values estimated from specimens of *Aulacopleura koninckii* (Table 1). Each column represents a trilobite at a different growth stage. The columns are arranged from earliest stage on the left to latest stage on the right. The blue section of each column represents the length of the cephalon, the gray-colored sections represent the thoracic tergites, and the pink section represents the length of the pygidium. (**C**) Schematic of trilobite body at molt 31; width of cranidium and pygidium set to be twice the length.
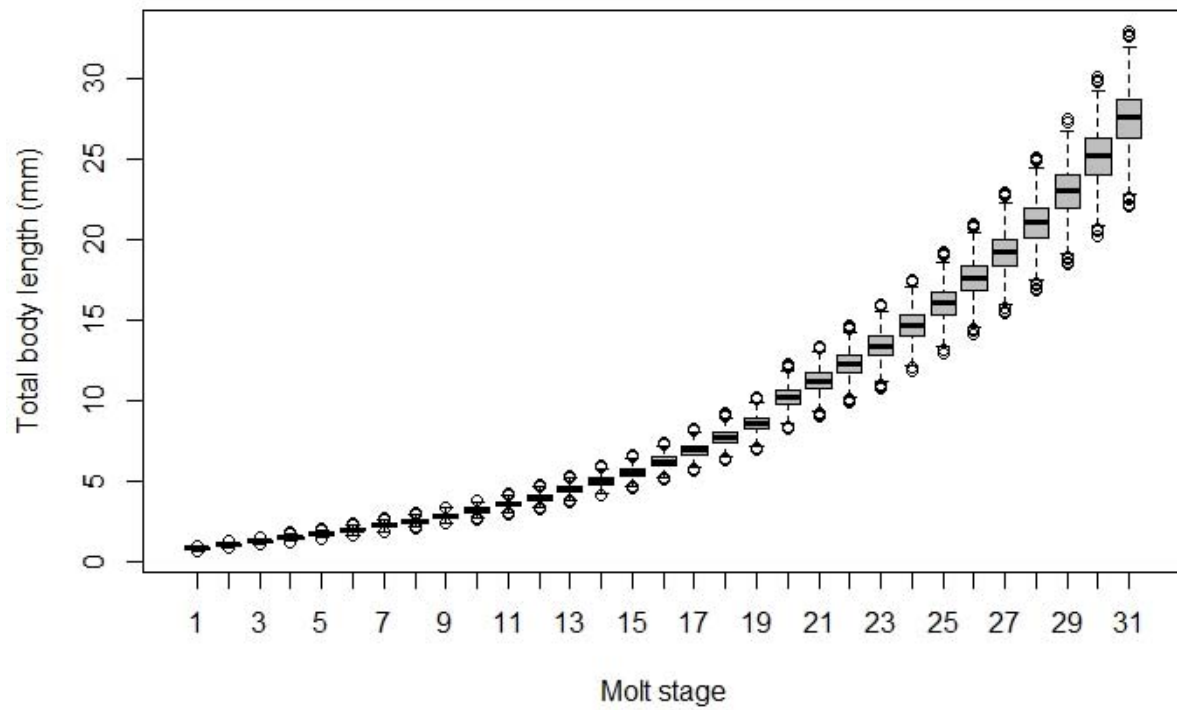
Figure 3. Variation in total body length at different stages when the lengths of the M0 cephalon and transitory pygidium are allowed to vary.
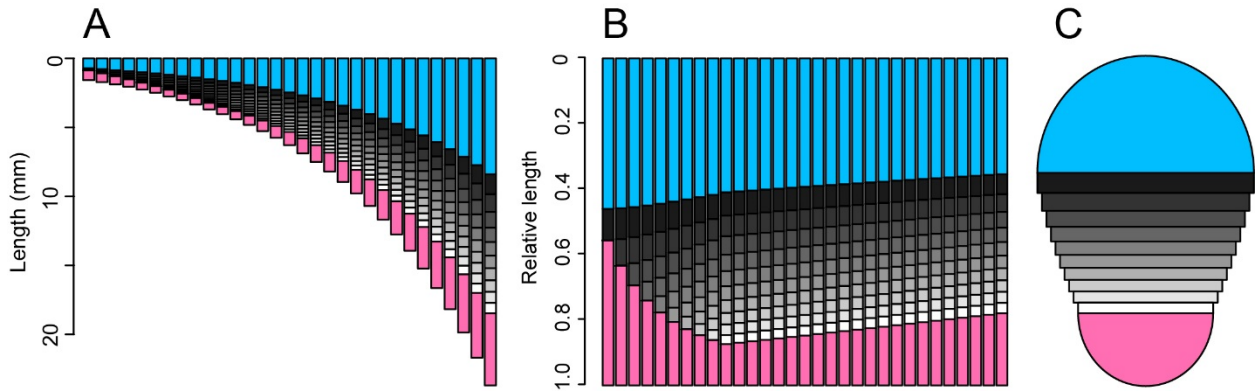
Figure 4. Model results when number of terminal tergites is varied. Estimated (**A**) and relative lengths (**B**) of dorsal sclerites for each molt (up to M = 31) when number of terminal tergites is decreased to 10 (all other parameters as in Table 1). (**C**) Schematic of trilobite body at molt 31; width of cranidium and pygidium set to be twice the length. Compared to *A. koninckii* with 20 terminal tergites (Figure 2, Table 2), the maximum body size (23.70 mm) is similar. Specifically, the trunk length is slightly decreased with much of the total length redistribution to the pygidium. The average tergite length is also longer. For color explanation, see Figure 2 caption.
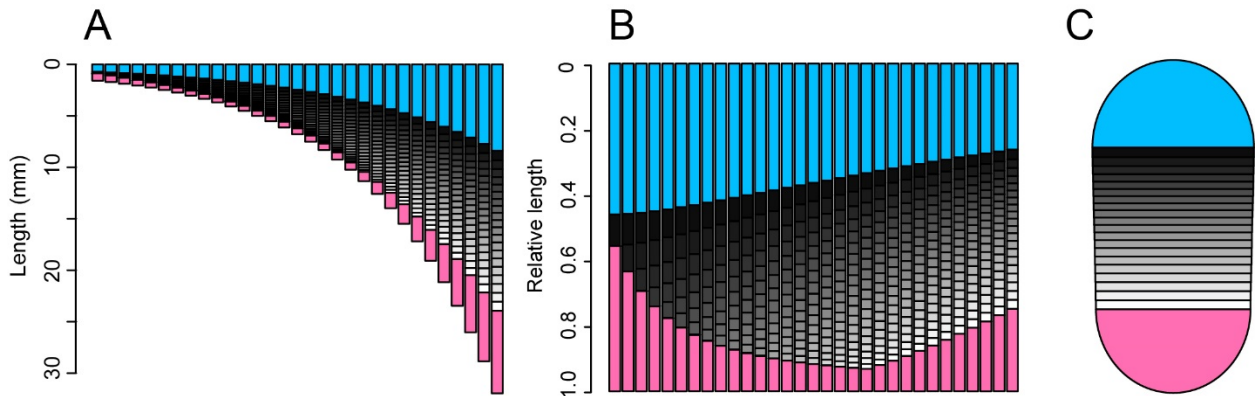
Figure 5. Model results if maximum growth rates near the posterior part of the trunk are maintained at higher values into the holaspid period. Here this is achieved by applying the same growth gradient in meraspid and holaspid periods (lowM = lowH = 1.059; highM = highH = 1.370; lambdaM = lambdaH = -5.001). (**A**) Estimated lengths of sclerites. (**B**) Relative lengths of sclerites. (**C**) Schematic of trilobite body at molt 31; width of cranidium and pygidium set to be twice the length. For color explanation, see Figure 2 caption.
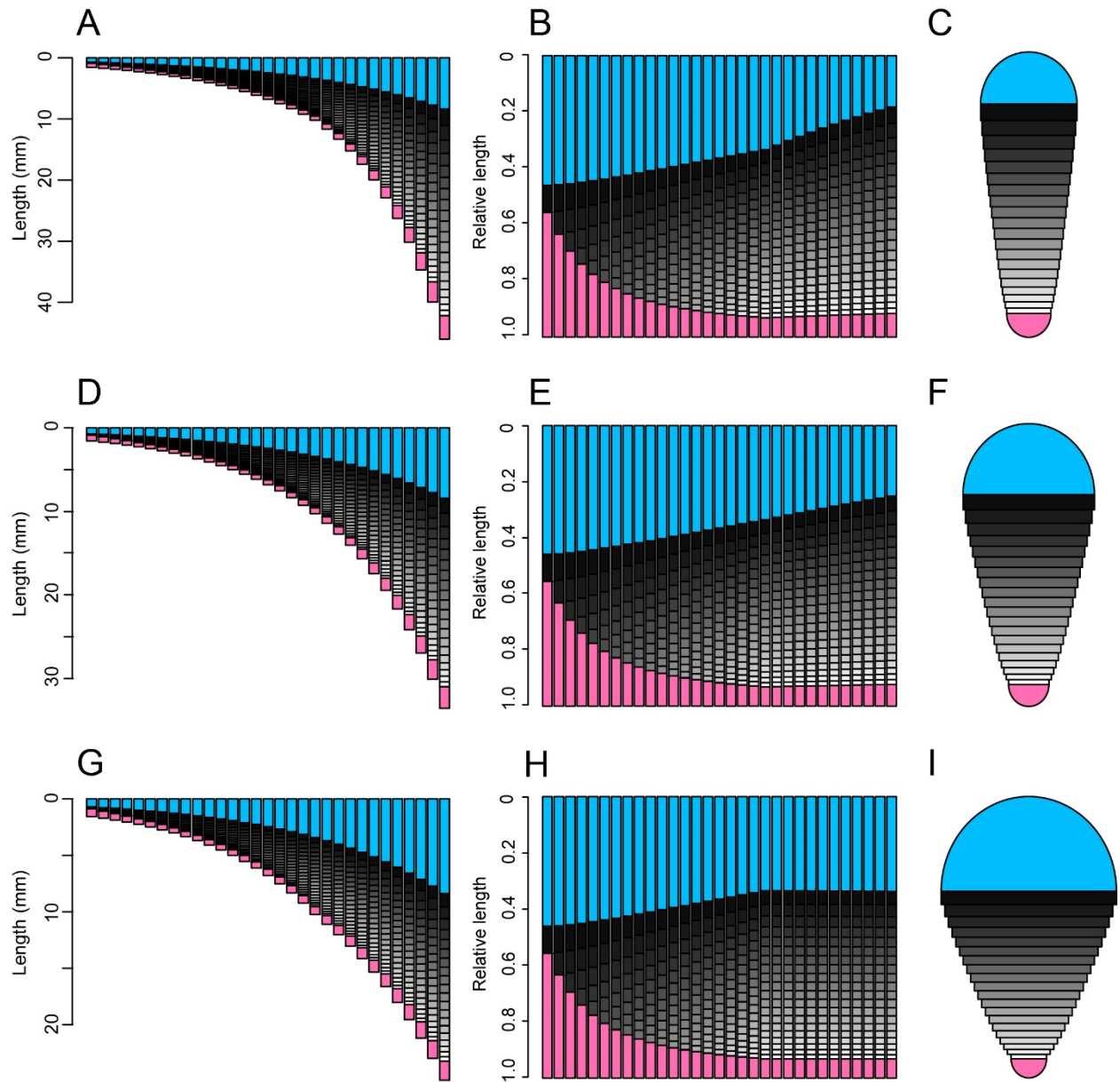
Figure 6. Growth patterns when constant rates are applied across the trunk region during the holaspid period. (**A-C**) Rates are close to the maximum expressed by *A. koninckii* during the holaspid period (*highH* = *lowH* = 1.168). (**D-F**) Rates are the average expressed by *A. koninckii* during the holaspid period (*highH* = *lowH* = 1.125). (**G-I**) Rates are the minimum expressed by *A. koninickii* during the holaspid period (*highH* = *lowH* = 1.084). For color explanation and further information about different columns, see Figure 2 caption.
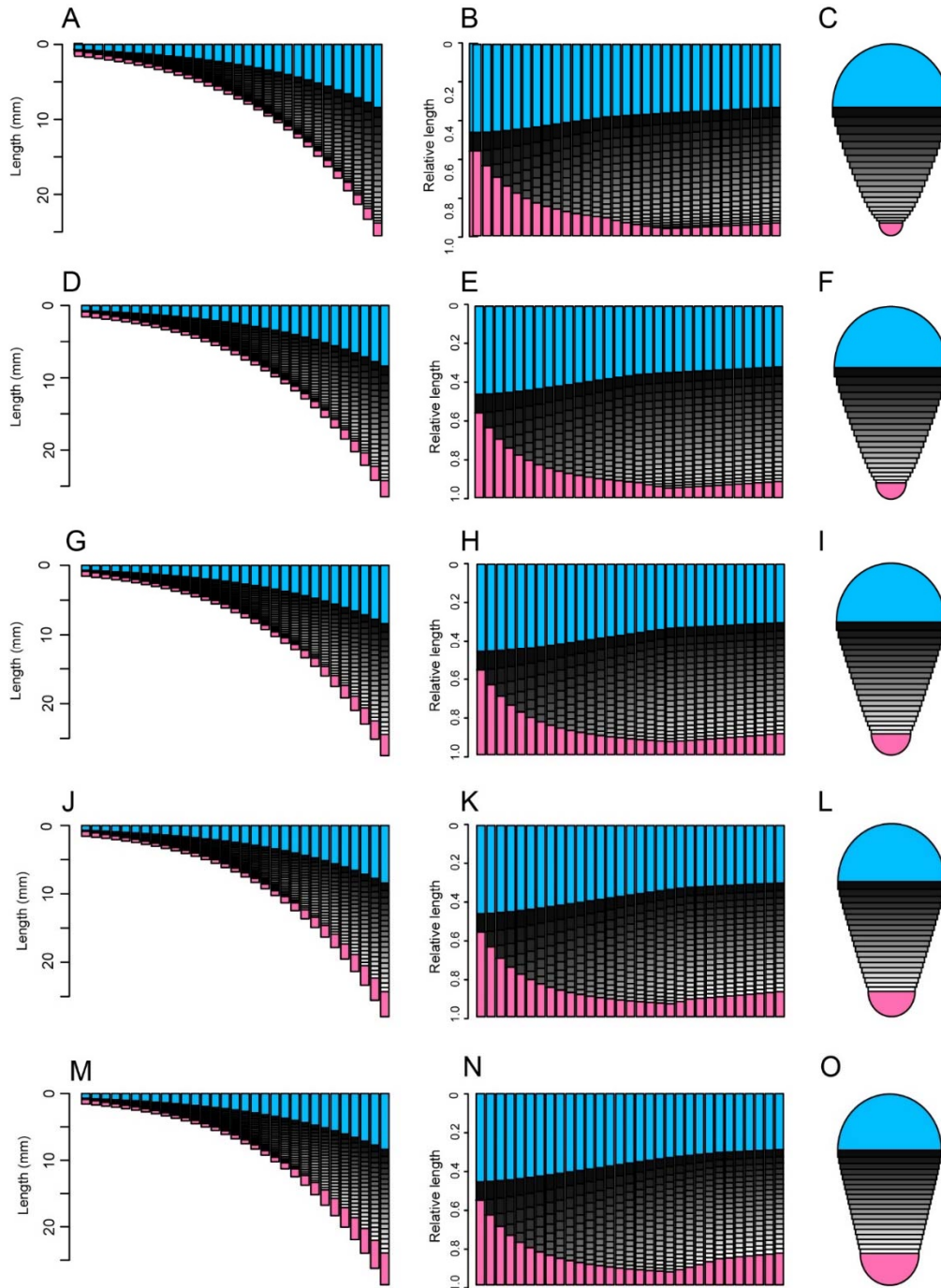
Figure 7. Impact of altering the relative timing of growth gradient transition and termination of tergite release into the thorax on body size and relative proportions. In all panels, termination of tergite release occurs at molt 20, but the transition from the initial growth gradient to the mature growth gradient R occurs in molt 15 (**A-C**), molt 18 (**D-F**), molt 20 (**G-I**), molt 22 (**J-L**), and molt 25 (**M-O**). The total exoskeletal length gets slightly longer going from the top to bottom panels but the relative proportion of the pygidium gets much longer at the expense of the total length of the thorax (the rate of cranidial growth is constant in all iterations). See also Table 3. For color explanation, see Figure 2 caption.
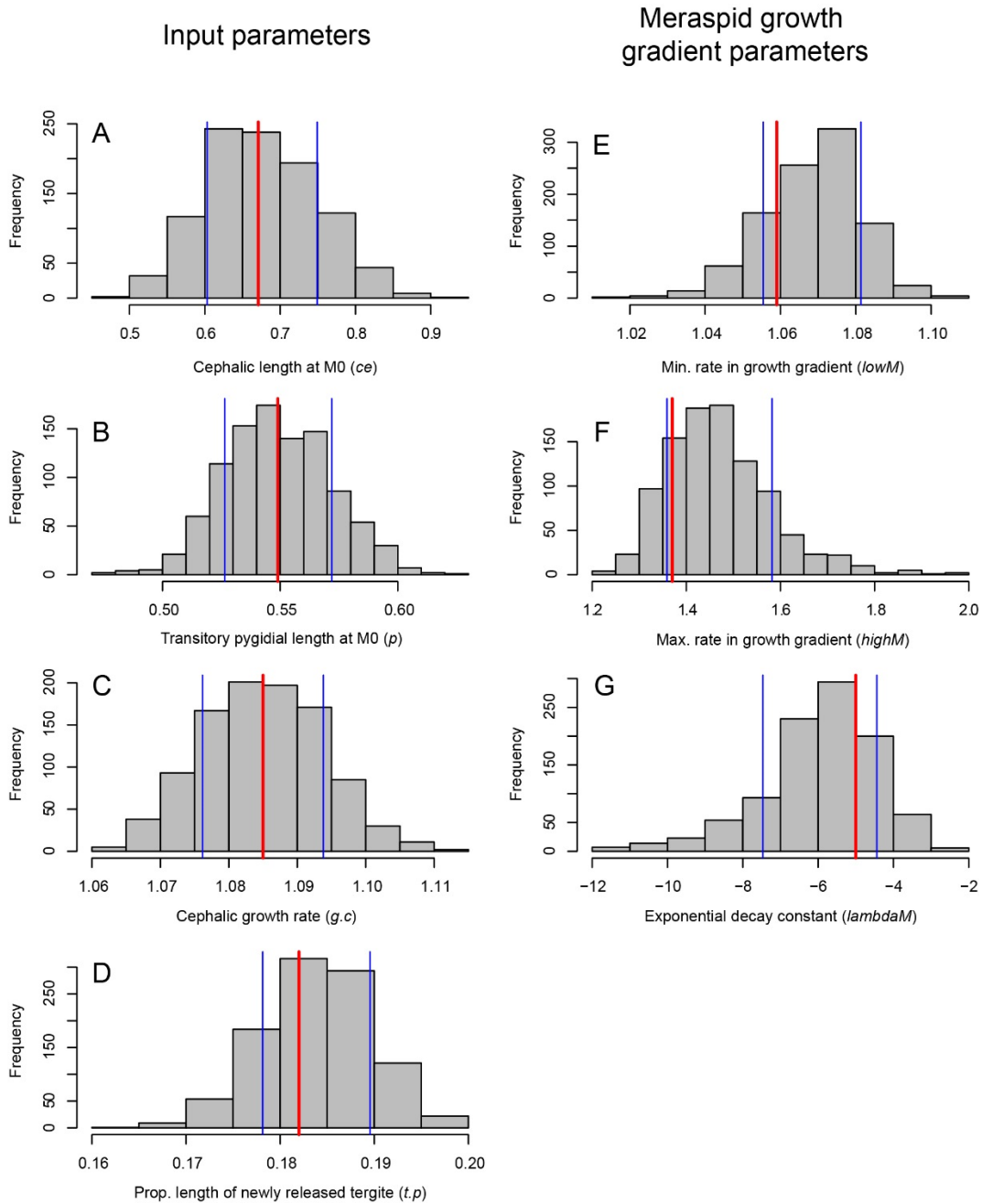
Figure 8. Parameters estimates for cephalic length at M0 (**A**), transitory pygidial length at M0 (**B**), cephalic growth rate (**C**), proportional length of newly released tergite (**D**), minimum rate in growth gradient (**E**), maximum rate in growth gradient (**F**), and exponential decay constant (**G**), calculated from subsets of *A. koninckii* specimens (one from each stage from M9 to M17). Blue lines show on standard deviation around the mean across all subsampled datasets. Red line shows the parameter estimated from the entire dataset (Table 1). For the growth gradient parameters, extreme outliers have been excluded: only maximum rates less than 2.0 (comprising 98.9% of the subsampling results) are shown; only exponential decay constants greater than -12 (comprising 98.5% of the subsampling results) are shown. See Figure 9 for complete ranges in estimates at low sample sizes.
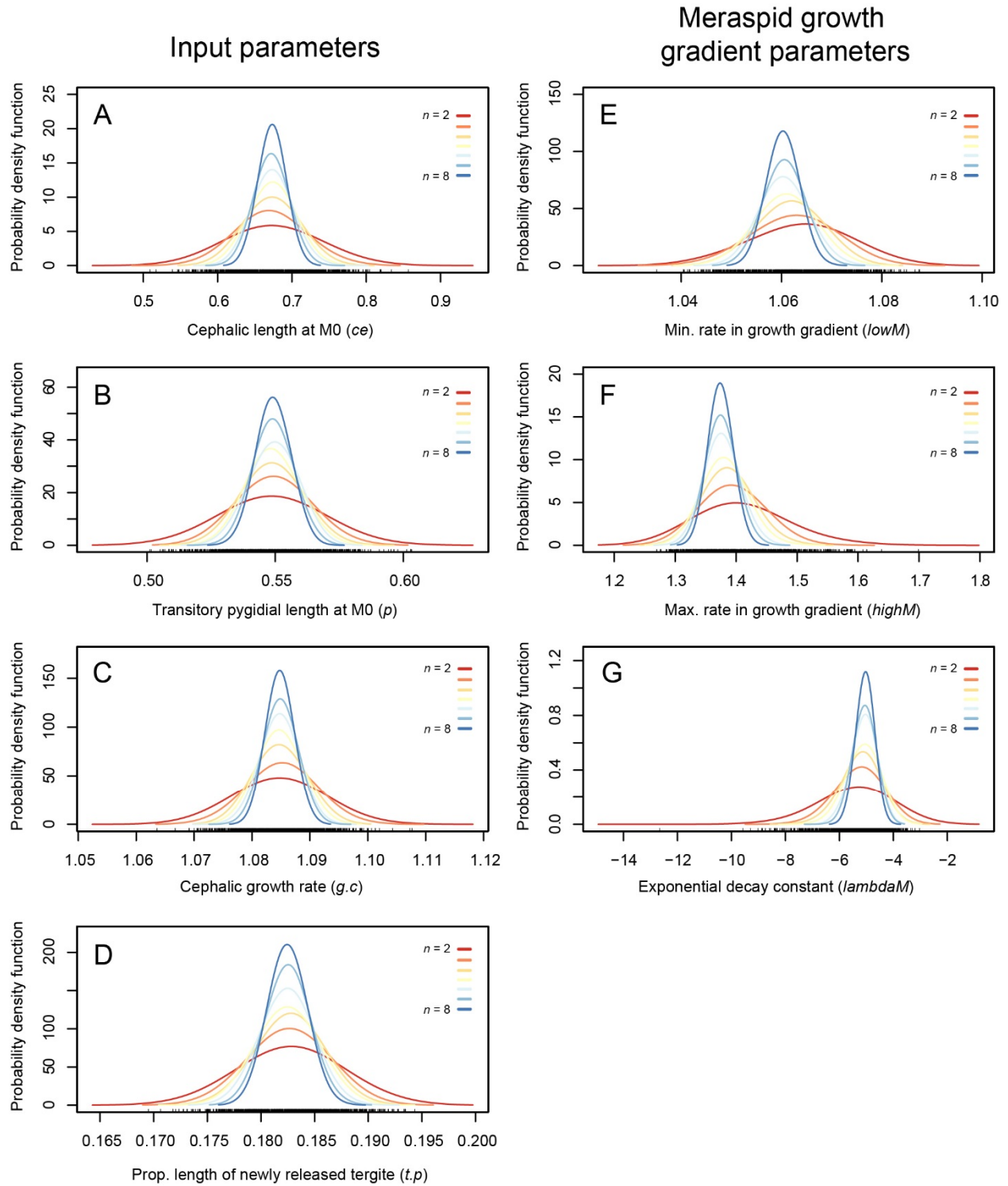
Figure 9. Parameters estimates for cephalic length at M0 (**A**), transitory pygidial length at M0 (**B**), cephalic growth rate (**C**), proportional length of newly released tergite (**D**), minimum rate in growth gradient (**E**), maximum rate in growth gradient (**F**), and exponential decay constant (**G**), calculated from subsets of *A. koninckii* specimens (two to eight specimens from each stage M9 to M17).
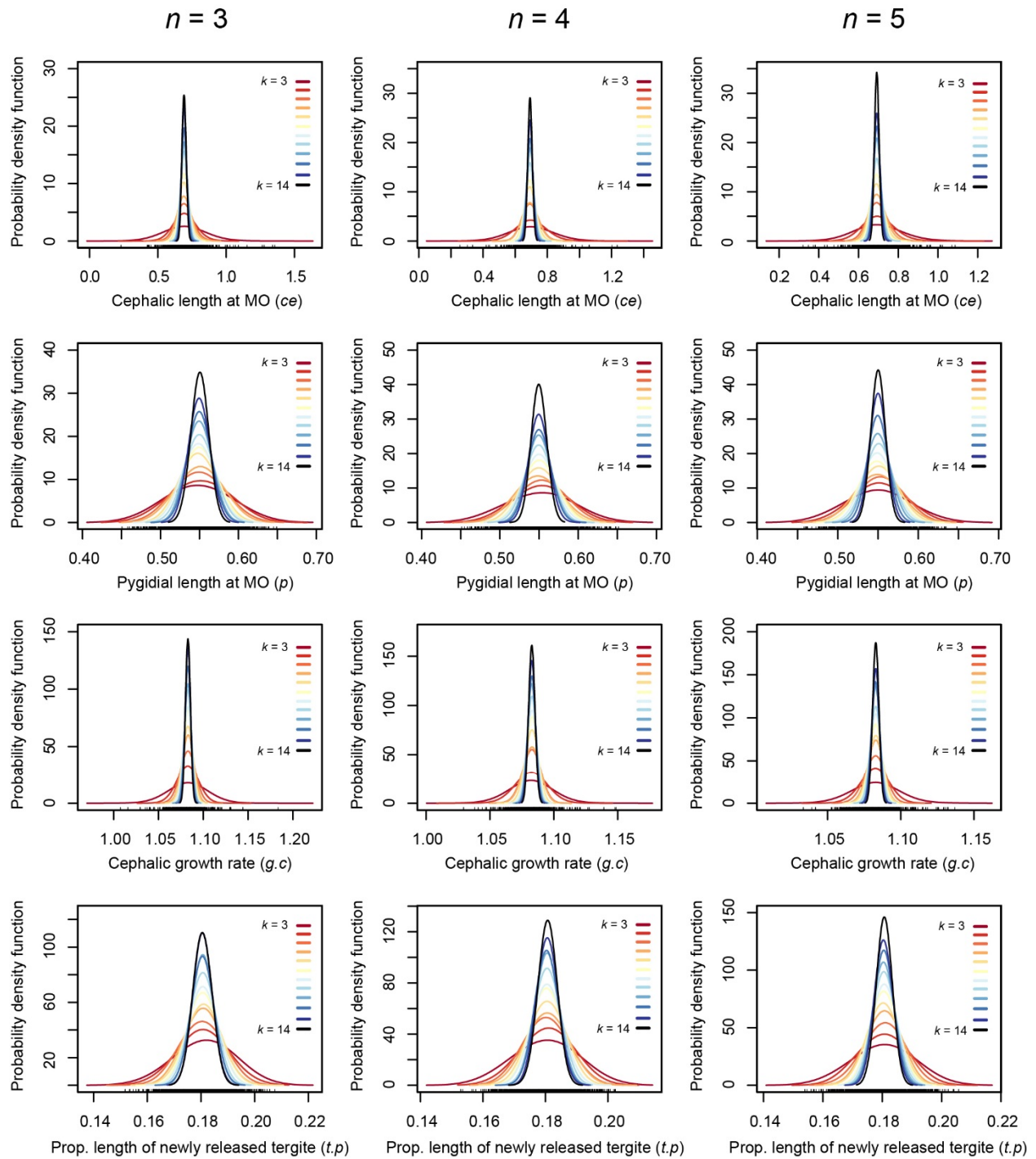
Figure 10A. Subsampling results for input parameter estimates when a few specimens (*n* ranges from 3 to 5) are randomly selected from a few to many (*k* ranges from 3 to 14) meraspid molt stages.
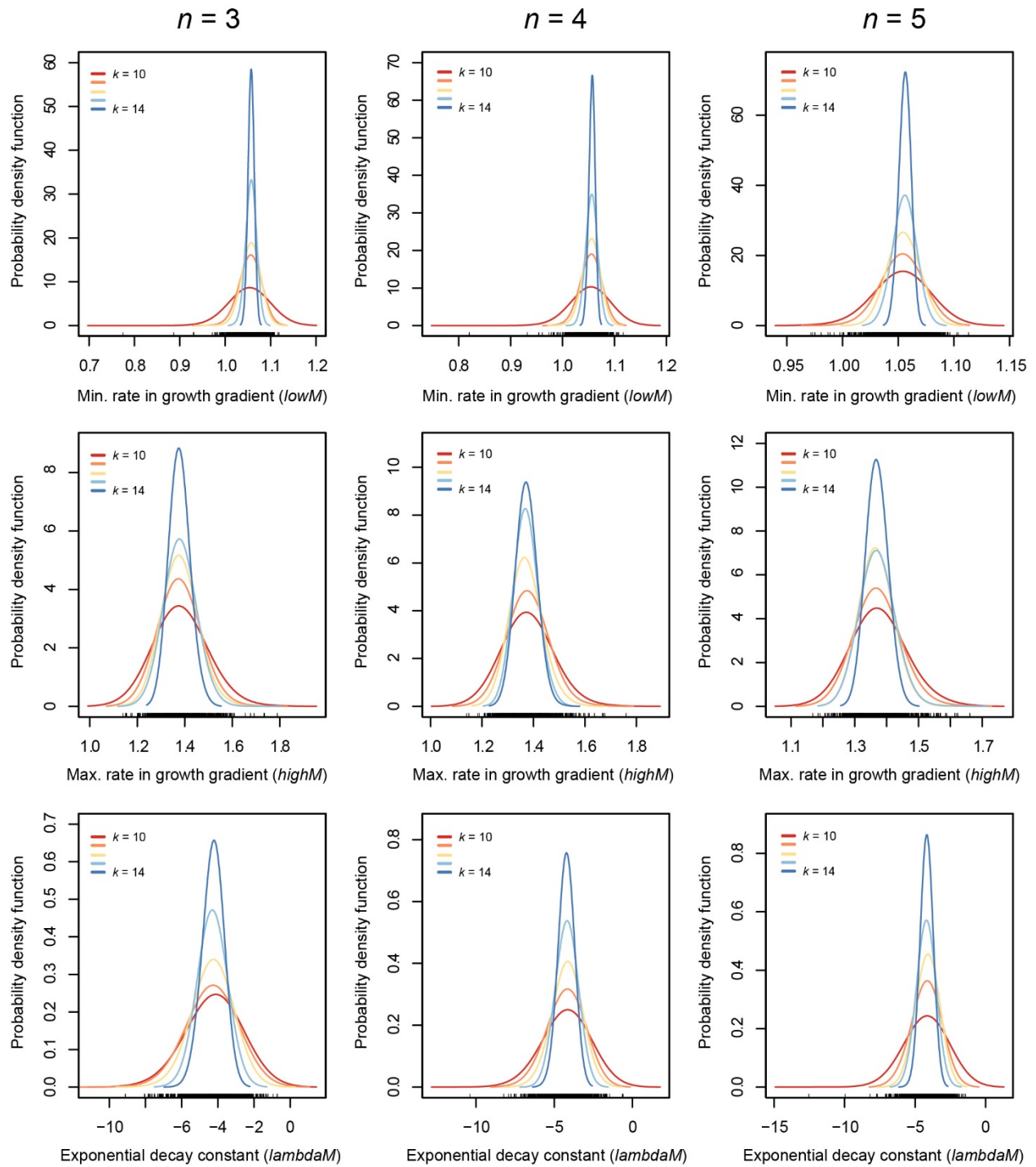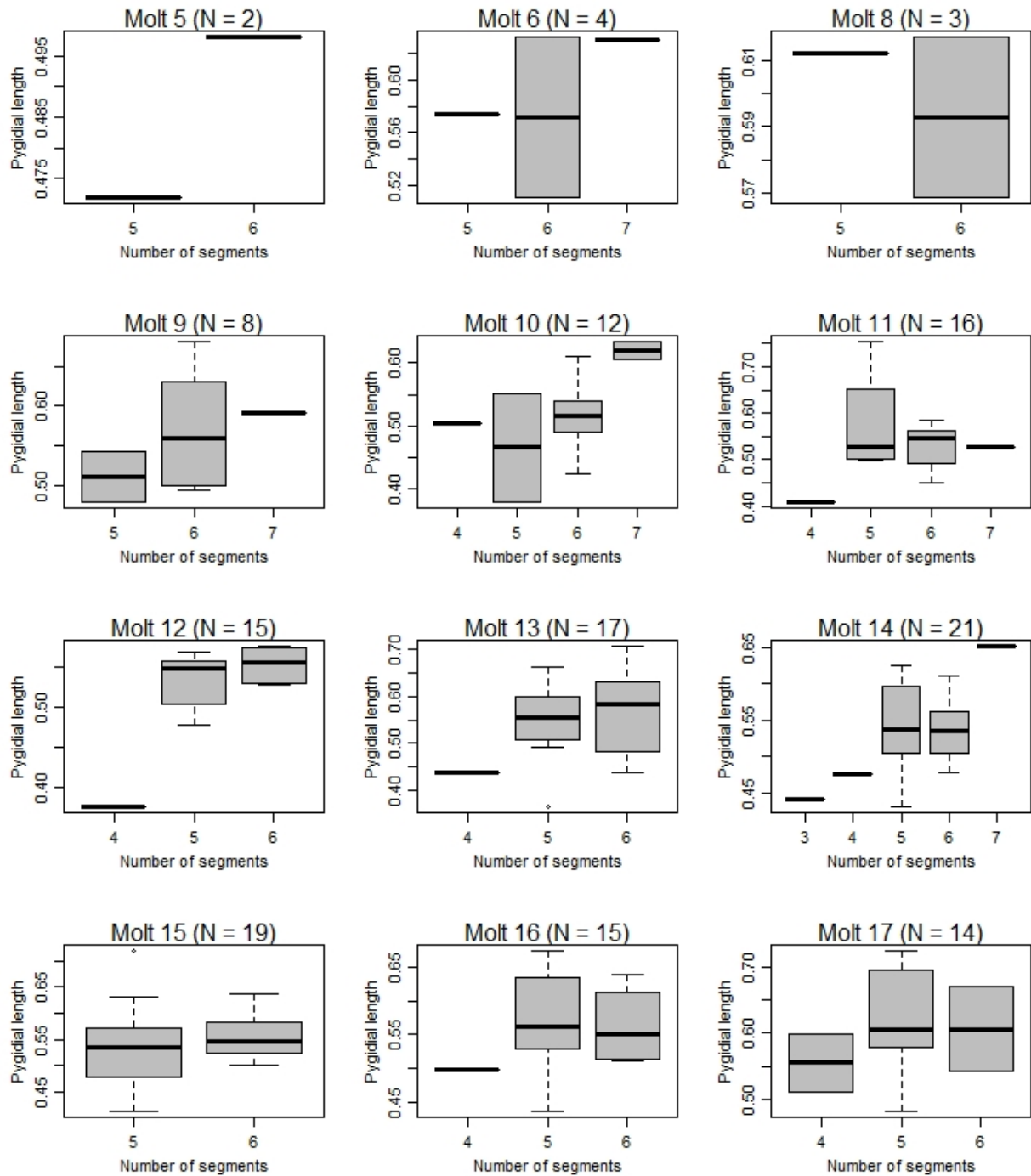
Figure 11. Subsampling results for growth gradient parameters when a few specimens (*n* ranges from 3 to 5) are selected from several to many (*k* ranges from 10 to 14) meraspid molt stages.

Supplementary Figure 1. Boxplots showing the range of pygidial lengths for each number of segments expressed in pygidia of that molt. Likelihood tests (G-tests) do not produce any statistically significant results.